Fusion of Regularization Terms For Image Restoration

Max Mignotte

***Abstract*— In this paper, we propose an efficient regularized restoration model associating a spatial and a frequential edge-preserving regularizers in order to better modeled the intrinsic properties of the original image to be recovered and to obtain a better restoration result. An adaptive and rescaling scheme is also proposed to balance the influence of these two different regularization constraints and allowing to prevent that a overwhelming importance for one of them prevail over the other in order to efficiently fuse them during the iterative deconvolution process. This hybrid regularization approach, mixing these two constraints and more precisely, favoring a solution image having simultaneously spatial sparseness of edges (with the GGMRF constraint) and sparseness of its frequency DCT coefficients, yields significant improvements in term of image quality and higher ISNR results, comparatively to a single GGMRF or DCT prior model, and leads to competitive restoration results, in benchmark tests, for various level of blur, BSNR and noise degradations.**

***Index Terms*— Regularized iterative restoration/deconvolution methods, edge-preserving regularizers, fusion of regularization terms, mix of multiple constraints, generalized Gaussian Markov random field (GGMRF) prior model, discrete cosine transform.**

I. Introduction

In regularized restoration approaches, the regularization term allows us to both to stabilize (from the computational viewpoint) the solution to the ill-conditioning restoration inverse problem and also to incorporate knowledge or beliefs concerning the types of restorations *a priori* defined as acceptable solutions. That is why the design of efficient image prior models or a priori regularization terms, and especially their ability to (locally and globally) summarize the intrinsic properties of the original image to be recovered are crucial in the final image quality and signal-to-noise improvement (ISNR) restoration result.

Over the last two decades, there have been considerable efforts to find an efficient regularization term capable of modeling the local image discontinuities, i.e., the edge model of a natural images. To this end, several edge-preserving regularization strategies were proposed (with some notable improvements in the restoration results) in the spatial [1]–[7] domain (*via* non-stationary, compound Markov model with possibly robust estimators) or in the frequential domain, by also promoting a restored image having a high sparsity of its spectral coefficients, *via* thresholding operations in the wavelet, Fourier or discrete cosine transforms [2], [5], [6], [8]–[13].

[1]Max Mignotte is with the Département d'Informatique et de Recherche Opérationnelle (DIRO), Université de Montréal, C.P. 6128, Succ. Centre-ville, H3C 3J7, Montréal (Québec). E-mail: mignotte@iro.umontreal.ca

To our knowledge, little attention has been given in associating/combining two different (but complementary) regularization terms and/or equivalently to propose a regularization strategy allowing to enforce simultaneously multiple (and different) constraints in order to improve the final restoration result. Nevertheless, some of the well known edge-preserving regularization priors are conceptually very different; either local and expressed in the spatial domain or more or less global and expressed in the (DCT, wavelet or Fourier) frequential domain. An hybrid regularization approach, mixing two or several of them, could efficiently better modeled the complex properties of the class of image *a priori* defined as acceptable solutions for a better final restoration result.

In this attempt to fuse several constraints or equivalently several prior knowledges for the image to be recovered, a Bayesian strategy has been recently proposed in [14], [15] which uses a statistical prior in product form. Such product type priors is able to combine multiple image prior models by assuming that the local discontinuities of the image (i.e., its edges) given by different local edge models (i.e., different high-pass filters) are Student-t distributed. In order to bypass the difficulty of evaluating the normalization constant of this product type prior, the authors in [14], [15] propose to use a constrained variational approximation methodology to infer the restored image.

The approach proposed in this paper is different and uses another fusion strategy. More precisely, our model simply exploits an additional constraint whose goal is to iteratively balance the influence of two (but possibly several) different penalty constraints, expressed by each image prior model, during a simple iterative Landweber deconvolution process. Besides, compared to [14], [15], our regularization strategy tends to enforce two different edge-preserving strategies, respectively expressed in the spatial and frequential domain, by promoting a restored solution having simultaneously spatial sparseness of edges, thanks to a GGMRF prior model and a restored solution having sparseness of its frequency DCT coefficients.

More generally, the concept of combining several classifiers, models or constraints for the improvement of the performance, or (in our application) to better modeled the complex properties of the class of image to be recovered by a restoration algorithm is known, in machine learning field, as a committee machine or mixture of experts [16], [17]. In this recent field of research, two major categories of committee machines are generally found in the literature. Our fusion approach is in the category of the committee machine model that utilizes an

ensemble of models or experts with a dynamic structure type. In this class of committee machines, the set of constraints are combined by means of a mechanism that involves the input data (contrary to the static structure type-based mixture of experts).

The remainder of this paper is organized as follows: Section II describes the proposed model with respectively the edge sparseness and the sparse representation constraints and finally the proposed fusion approach of these two constraints in an iterative deconvolution Landweber process. Finally, section III presents a set of experimental results and comparisons with existing restoration techniques.

II. Proposed Approach

A. Edge Sparseness Constraint In The Spatial Domain

The first regularization term used in our restoration model is formulated in the (image) spatial domain and allows to promote a (regularized) restored image $\hat{x}$ with spatial smoothness and edge sparsity properties. To this end, we have considered the GGMRF prior model proposed by Bouman *et al.* in tomographic reconstruction [18], [19]. This prior has a density function of the form $P_X(x) \propto \exp\{-\gamma\,\Omega(x)\}$ with the following regularization term

$$\Omega(x) = \sum_{<s,t>} \beta_{st} |x_s - x_t|^q \tag{1}$$

where $1 \leq q \leq 2$ is a parameter controlling the smoothness of the image to be recovered and/or the sharpness of the edges to be formed in the restored image. $\beta_{st} = (2\sqrt{2}+4)^{-1}$ or $(4+4\sqrt{2})^{-1})$ depends on whether the pair of neighboring sites (relative to the second order neighborhood system), or binary clique $<s,t>$ is horizontal/vertical or right diagonal/left diagonal. This prior model has the advantage to include a Gaussian MRF prior for $q=2$ and a more interesting edge-preserving absolute-value potential function with $q=1$. In the regularization framework and under this first constraint a restored image can be seen as a solution to the following penalized likelihood cost function to be optimized

$$\hat{x} = \arg\min_x \Big\{ \|y - h * x\|^2 + \gamma\,\Omega(x) \Big\} \tag{2}$$

where y and x represent respectively, the observed blurred and noisy image (degraded by an additive and white Gaussian noise with variance σ^2) and the undistorted true image. h is the Point Spread Function (PSF) of the imaging system[2] and $*$ is the linear convolution operator. For the convolution procedure, we herein assume that the image is toroidal, i.e., periodically repeated. The first term of this cost function expresses the fidelity to the available data y and the second encodes the spatial smoothness and the local edge-sparsity constraint (i.e., the expected properties) of the true undegraded image. γ is the regularization parameter controlling the contribution of the two terms. A maximum penalized likelihood estimate of the undegraded image $\hat{x}$, under this GGMRF constraint, can be found by a classical gradient descent method. To this end, the derivative of $\Omega(x)$ at site s, has the following analytical expression $\Omega'(x_s) = q \sum_{<s,t>} \beta_{st} |x_s - x_t|^{q-1} \text{sign}(x_s - x_t)$ and leads to the following iterative steepest descent procedure, which moves the penalized likelihood estimates in the negative gradient direction

$$\hat{x}^{[n+1]} = \underbrace{\hat{x}^{[n]} + \alpha^{[n]}\, h^{\#} * (y - h * \hat{x}^{[n]}}_{\hat{x}_{\text{ML}}^{[n]}} - \gamma\,\Omega'(\hat{x}^{[n]}) \tag{3}$$

where $h^{\#}(i,j) = h(-i,-j)$ (the coordinates (i,j) represent the discrete pixel locations and for h symmetric, we have $h^{\#} = h$). After derivation of Eq. (2), $\alpha^{[n]}$ is a constant equals to 1 for all n. Nevertheless we can easily speed up this iterative search procedure by adaptively changing $\alpha^{[n]}$ at each iteration according to the following equations [20]

$$\alpha^{[n]} = \frac{\|q^{[n]}\|^2}{\|h * q^{[n]}\|^2} \quad \text{with} \quad q^{[n]} = h^{\#} * (y - h * \hat{x}^{[n]}) \tag{4}$$

where, in this notation, pixels are organized in $q^{[n]}$ and in $h * q^{[n]}$ in lexicographic order as one large column-vector. For $\gamma = 0$, the iterative procedure defined in Eq. (3) is the (accelerated) well known Landweber algorithm [21].

B. Sparsity Constraint In The Frequential Domain

The second constraint used in our restoration model is formulated in the Discrete Cosine Transform (DCT) domain by promoting a restored image having a high sparsity in the (DCT) frequency domain. To this end, a convenient way to impose this constraint, i.e., to enforce the sparseness of the DCT coefficients w_i on the restored image consist in applying to each of these coefficients (of each individual block of size 8×8 pixels of $\hat{x}^{[n]}$), a simple thresholding operation. An example of sparsity constraint in the (frequency domain is the so-called soft-thresholding operation classically used in the wavelet based denoising approach [13], [22], [23]) of each DCT coefficients, according to the following rule

$$\lambda_T^{\text{soft}} = \text{sgn}\,(w)(|w| - T)_+ \tag{5}$$

where $(.)_+$ is defined as $(x)_+ = \max\{x, 0\}$ and sgn(.) is the sign function (sgn$(x) = 1$, if $x \leq 0$, and sgn$(x) = -1$, otherwise). Another example is the hard version of this soft-thresholding operation, leading to the following hard - thresholding rule

$$\lambda_T^{\text{hard}} = \begin{cases} 0 & \text{if} \quad |w| \leq T \\ w & \text{otherwise} \end{cases}$$

in which T is a threshold level that acts as a regularization parameter and we recall that w is one of the coefficients obtained by the DCT transform of the block (of size 8×8 pixels) extracted from the current image estimate. These two thresholding rules allows to enforce the *a priori* sparse representation (in the DCT domain) of the solution image to be recovered, or equivalently allows to favor a generalized Gaussian law for the distribution of these DCT coefficients [23].

[2]We shall assume throughout this paper that the degradation model (PSF and variance of the white Gaussian noise) is known. It might be given analytically or given numerically based on previous estimations or calibration experiments.

In order to reduce blocky artifacts across the 8×8 block boundaries, a standard way (already used in the wavelet denoising community) is to make this transform translation-invariant, i.e., to use the DCT of all (circularly) translated version of the image herein assumed to be toroidal [24], [25]. This thus implies (for a set of 8×8 blocks extracted from the image) to compute a set of 8 horizontal shifts and 8 vertical shifts ($= 64$) translated images which will then be DCT-denoised with the soft or hard thresholding rule and then averaged in a final step (see Algorithm 1).

DCT-Based Denoising Step

$x^{[n]}$ Input image to be denoised at iteration n
$\hat{x}^{[n]}$ Denoised estimated image at iteration n
T Threshold

for *All (*8 *horiz. and* 8 *vert.) shifts of* $x^{[n]}$ **do**
  for *All* $[8 \times 8]$ *blocks extracted from* $x^{[n]}$ **do**
    1. DCT Transform
    2. Threshold the obtained DCT coefficients w with the hard thresholding rule

$$\lambda_T^{\text{hard}} = \begin{cases} 0 & \text{if } |w| \leq T \\ w & \text{otherwise} \end{cases}$$

    or the soft thresholding rule

$$\lambda_T^{\text{soft}} = \text{sgn}\,(w)(|w| - T)_+$$

    3. Inverse DCT of these thresholded coef.
  ▷ Unshift the filtered image and store it

$\hat{x}^{[n]} \leftarrow$ Averaging of these 64 denoised images

Algo 1 : DCT-Based Denoising Step ($\Upsilon_{\text{T}}(x^{[n]})$)

C. Fusion of Regularization Terms

The goal of this work is to propose a restoration procedure which promotes an acceptable restored image combining these two above-mentioned sparseness constraints, i.e., favoring a solution image having simultaneously spatial sparseness of edges (with the GGMRF constraint) and sparseness of its frequency DCT coefficients while ensuring the likelihood fidelity, i.e., by finding an estimate $\hat{x}$ ensuring an acceptable minimum for the likelihood energy $\|y - h * x\|^2$ under these two constraints. Equivalently, we would like to restrict the types of restorations (*a priori*) defined as acceptable solutions as those combining these two complementary spatio-frequential sparseness constraints.

The problem is not trivial since, the simple solution which would consists in alternating the two regularization strategies, i.e., an iteration of the gradient descent of the penalized likelihood function (Eq. (3)) followed by a DCT denoising step (Algo. 1) leads to restoration results equal to those obtained in the case of the only use of the GGMRF regularization term or of the DCT-based constraint, according to the value given to the two regularization parameters (i.e., γ for the GGMRF regularization term and T for the DCT constraint).

A rescaling problem, inherent to the fusion of these two regularization terms exist and must herein be treated. To this end, we have thus to balance the influence of these two different regularization strategies (in the sense of a criterion or another constraint), during the iterative search process of the solution image. This rescaling will allow to prevent that a overwhelming importance for one of the two regularization constraints prevail over the second (and thus making the fusion of the two regularization terms inefficient). This rescaling problem is somewhat identical to the one occurring in pattern classification when different features with different units are blended together. In this case, the rescaling step prevents that the similarity measure (used to evaluate the distance between feature vectors) will (wrongly) give an overwhelming importance to feature having a larger unit range.

In this work, in order to prevent that a overwhelming importance for one of these two penalty terms prevail over the second (and thus making the fusion of these two regularization strategies inefficient), we decide to adaptively balance the two regularizers by adding, to the iterative search process of the restored image, the following adaptive empirical constraint:
"*The residual image added to the likelihood image, to each iteration of the iterative search process, by the GGMRF based constraint and the DCT based constraints should be equal in a norm sense.*"
In our application, the likelihood image ($\hat{x}_{\text{ML}}^{[n]}$) is the solution image obtained at iteration n, without the n^{th} constraint, i.e., the image obtained by Eq. (3) with $\gamma^{[n]} = 0$. The residual image designates the additive correction image added (at each iteration) to the likelihood image by the presence of each constraint. In the case of the GGMRF constraint, the regularization adds, at iteration n, to the image likelihood the corrective term $\|\gamma^{[n]}\, \Omega'(\hat{x}^{[n]})\|$ (see Eq. (3)). In the case of the DCT-based denoising constraint (without the GGMRF-constraint), this residual image is simply (at each iteration n) the difference image between the DCT-denoised likelihood image minus the likelihood image, i.e., $\|\Upsilon_T(\hat{x}_{\text{ML}}^{[n]}) - \hat{x}_{\text{ML}}^{[n]}\|$. In this expression, $\Upsilon_T(.)$ designates the [DCT-THRESHOLDING-INVERSEDCT] operator with the thresholding operation according to the rule given by Equations (6) or (5) with the regularization parameter value T.

The following section used this additional constraint in order to adaptively estimate $\gamma^{[n]}$ as a function of T during the iterative search restoration procedure.

D. Parameter Estimation

In our restoration model, T is preliminary and empirically set according to the noise standard variation σ of the considered degradation model by the following procedure

$$T_{\text{Hard}} = \begin{cases} 1.6\,\sigma & \text{if} \quad \sigma^2 < 10 \\ 2.2\,\sigma & \text{if} \quad \sigma^2 \geq 10 \end{cases} \tag{6}$$

or, for the soft thresholding rule, by

$$T_{\text{Soft}} = \begin{cases} 0.2\,\sigma & \text{if} \quad \sigma^2 < 10 \\ 0.6\,\sigma & \text{if} \quad \sigma^2 \geq 10 \end{cases} \tag{7}$$

$\gamma^{[1]}$ is then estimated at the first iteration of our restoration algorithm and adaptively change in order to adaptively balance

(for each iteration of our iterative algorithm) the residual image added to the likelihood image between the two sparseness constraints. Given T, $\gamma^{[n]}$ is thus estimated by

$$\hat{\gamma}^{[n]} = \arg\min_{\gamma}\left\{\left|\underbrace{\left\|\Upsilon_T(\hat{x}_{\text{ML}}^{[n]}) - \hat{x}_{\text{ML}}^{[n]}\right\|_1}_{\mathcal{B}_{\text{DCT}}} - \underbrace{\left\|\gamma^{[n]}\,\Omega'(x^{[n]})\right\|_1}_{\mathcal{B}_{\text{GGMRF}}}\right|\right\} \tag{8}$$

where $\|.\|_1$ is the $\mathcal{L}1$-norm and $\mathcal{B}_{\text{DCT}}$ and $\mathcal{B}_{\text{GGMRF}}$ represent respectively the residual image added to the likelihood at each iteration of the restoration process. In our application, $\gamma^{[n]}$ is estimated by a dichotomy search algorithm based on the sign of $(\mathcal{B}_{\text{DCT}} - \mathcal{B}_{\text{GGMRF}})$. We stop the procedure when the relative distance between two successive values is less than 10^{-3}. During the iterative restoration procedure, $\gamma^{[n]}$ is then refined, at each step n of the iterative restoration process, with the following procedure

$$\gamma^{[n+1]} = \begin{cases} 0.95\,\gamma^{[n]} & \text{if} \quad \mathcal{B}_{\text{GGMRF}} > \mathcal{B}_{\text{DCT}} \\ 1.05\,\gamma^{[n]} & \text{otherwise} \end{cases} \tag{9}$$

1) Estimation of Number of Iterations: The convergence criterion of the proposed restoration procedure is empirically defined by

$$\text{Number of iterations} = \max\left\{400, \frac{1500}{\sigma^2}\right\} \tag{10}$$

III. Experimental Results

A. Set Up

For the implementation of the DCT-based denoising step, we have used the fast 8×8 FFT2D DCT package implemented in C code by Takuya Ooura (functions DDCT8X8S tested in program SHRTDCT.C) and available on-line at http address given in [26].

In order to compare the efficiency of our restoration model using a regularization term fusion-based procedure, comparatively to a restoration model using a single GGMRF or DCT prior model, we have thus considered, for comparisons :

1) The restoration algorithm using only the GGMRF prior model ($q = 1$). In this case, the regularization parameter γ, that controls the contribution of the likelihood and prior terms is given by $\gamma = \sigma^2/6.0$, which ensures (after several trials and errors) a nearly optimal restoration results for all the experiments tested in this paper.
2) The restoration procedure using only the DCT-based complexity prior model. More precisely, this procedure simply leads to the iterative Landweber [21] procedure (Eq. (3) with $\gamma = 0$) whose each iterative step is regularized by the DCT denoising step (using the hard thresholding rule and the estimation procedure given by Eq. (6)). For our tests, this algorithm is called the "DCT-gradient".
3) The proposed restoration method (summarized in pseudo code in Algorithm II), i.e., the combined GGMRF$_{q=1}$ and DCT-based (with the hard thresholding rule) denoising constraints with the adaptive scheme to weight the two different regularization terms and the parameter estimation procedure given by Equations (6), (8), (9) and (10).

GGMRF-DCT-based restoration algorithm

σ^2	Variance of the noise
T	Threshold value of the sparsity constraint
Υ_T	DCT denoising (see Algo I)
γ	Regularization value of the GGMRF model

$$T = \begin{cases} 1.6\,\sigma & \text{if} \quad \sigma^2 < 10 \\ 2.2\,\sigma & \text{if} \quad \sigma^2 \geq 10 \end{cases}$$

1. Estimation of $\hat{\gamma}^{[0]}$

$$\hat{\gamma}^{[0]} = \arg\min_{\gamma}\left\{\left|\left\|\Upsilon_T(\hat{x}_{\text{ML}}^{[0]}) - \hat{x}_{\text{ML}}^{[0]}\right\|_1 - \left\|\gamma\,\Omega'(\hat{x}^{[0]})\right\|_1\right|\right\}$$

with $\quad \hat{x}_{\text{ML}}^{[n]} = \hat{x}^{[n]} + \alpha_n\, h^{\#} * (y - h * \hat{x}^{[n]})$

$$\alpha^{[n]} = \frac{\|q^{[n]}\|^2}{\|h * q^{[n]}\|^2} \quad \text{and} \quad q^{[n]} = h^{\#} * (y - h * \hat{x}^{[n]})$$

by using a dichotomy search algorithm

2. Restoration

while $n < \max\left\{400, \frac{1500}{\sigma^2}\right\}$ **do**

- if n is odd

$$\hat{x}^{[n+1]} \leftarrow \hat{x}^{[n]} + \alpha^{[n]}\, h^{\#} * (y - h * \hat{x}^{[n]}) - \gamma^{[n]}\,\Omega'(\hat{x}^{[n]})$$

- if n is even

$$\hat{x}^{[n+1]} \leftarrow \Upsilon_T(\hat{x}_{\text{ML}}^{[n]})$$

Iterative rescaling of $\hat{\gamma}^{[n+1]}$ ▶

$$\hat{\gamma}^{[n+1]} = \begin{cases} 0.95\,\hat{\gamma}^{[n]} \\ \text{if} \quad \left\|\hat{\gamma}^{[n]}\,\Omega'(\hat{x}^{[n]})\right\|_1 > \left\|\Upsilon_T(\hat{x}_{\text{ML}}^{[n]}) - \hat{x}_{\text{ML}}^{[n]}\right\|_1 \\ 1.05\,\hat{\gamma}^{[n]} \quad \text{otherwise} \end{cases}$$

$n \leftarrow n + 1$

Algo 2 : GGMRF-DCT-based restoration algorithm

B. Comparison with State-of-the-art Methods

We now present a set of experimental results and comparisons illustrating the performance of the proposed approach. To this end, we have replicated the degradation models generally used by several authors and we have compared the ISNR result given by our approach and the other published state-of-the-art methods respectively in Tables II and III. In these experiments, original images are CAMERAMAN (experiments 1, 2, 3, 5 and 6) of size 256×256 and LENA of size 512×512 (experiment 4). Table I summarizes the different degradation models used, which are defined by the blur type, the variance of the additive white Gaussian noise and the resulting BSNR (i.e., the ratio between the variance of the noise and the variance of blurred image without noise) for each of the experiments. The best ISNR results provided by the existing restoration algorithms

Fig. 1. From top to bottom, original image, Noisy-blurred image for Exp1 (see Table I) and restored image using the proposed restoration approach ISNR=9.02 dB (see Table II).

Fig. 2. From top to bottom, original image, Noisy-blurred image for Exp3 (see Table I) and restored image using the proposed restoration approach ISNR=5.33 dB (see Table II).

and the results provided by our approach for each degradation level are indicated in bold.

C. Comparison with the SA-DCT regularized deconvolution

Since the SA-DCT deconvolution algorithm proposed by Foi *et al.* in [2] also uses a DCT-based denoising step, a comparison and a discussion is herein given in what concerns difference of models, estimation/sensitivity of the internal parameters and computational complexity of the two restoration methods. The SA-DCT regularized deconvolution algorithm proposed in [2] is a non-iterative two-step restoration procedure whose first step is essentially a deblurring stage given by a regularized Wiener filtering. The second step is a DCT filtering, applied on this resulting deblurred image, computed on several polygonal supports whose shape are defined by a preliminary segmentation technique (called LPA-ICI for

TABLE I

BLUR, NOISE VARIANCE AND BSNR (DB) FOR EACH EXPERIMENT

	Blur	σ^2	BSNR
Exp1	9×9 uniform [CAMERAMAN 256×256]	.308	40
Exp2	$h_{ij}=(1+i^2+j^2)^{-1}$, $i,j=-7,\ldots,7$ [CAMERAMAN 256×256]	2	32
Exp3	$h_{ij}=(1+i^2+j^2)^{-1}$, $i,j=-7,\ldots,7$ [CAMERAMAN 256×256]	8	26
Exp4	$[1,4,6,4,1]^t[1,4,6,4,1]/256$ [LENA 512×512]	49	16.5
Exp5	5×5 uniform [CAMERAMAN 256×256]	33.3	20
Exp6	$\propto[1+(i^2+j^2)/16]^{-3}$ $i,j=-9,\ldots,9$ [CAMERAMAN 256×256]	62.5	17

TABLE II

PERFORMANCE COMPARISON BETWEEN OUR ALGORITHM AND OTHER RESTORATION METHODS FOR EXPERIMENTS EXP1-4

	ISNR (dB)			
Methods	Exp1	Exp2	Exp3	Exp4
GGMRF-DCT-gradient	**9.02**	**7.76**	**5.33**	**4.48**
DCT-gradient	8.10	7.01	5.13	4.14
GGMRF-gradient	7.64	6.71	4.61	2.59
(2009) Oliveira *et al.* [7]	8.60	5.18	**7.42**	2.78
(2008) Dabov *et al.* [27]	8.34	-	-	**4.81**
(2008) Chantas *et al.* [15]	**9.53**	-	-	3.03
(2008) Mignotte [4]	7.81	7.14	5.24	3.84
(2007) Chantas *et al.* [14]	9.16	-	-	3.58
(2007) Babacan *et al.* [28]	8.39	-	-	-
(2006) G.-Colon & Portilla [8]	7.33	7.45	5.55	-
(2006) Bioucas-Dias *et al.* [9] [10]	8.52	-	-	2.97
(2006) Chantas *et al.* [1]	8.91	-	-	3.77
(2006) Foi *et al.* [2]	8.58	**8.29**	6.34	4.55
(2006) Mignotte [3]	8.23	7.58	5.70	1.63
(2006) Bioucas-Dias [12]	8.10	7.40	5.15	2.85
(2005) Figueiredo & Nowak [11]	8.16	7.46	5.24	2.84
(2004) Katkovnik *et al.* [29]	8.23	-	-	-
(2004) Neelamani *et al.* [5]	7.30	-	-	-
(2003) Figueiredo & Nowak [13]	7.59	6.93	4.88	2.94
(2001) Jalobeanu *et al.* [30]	-	6.75	4.85	-
(1998) Liu & Moulin [31]	-	-	-	1.08
(1996) Banham & Katsaggelos [6]	6.70	-	-	-

local polynomial approximation - intersection of confidence intervals). To summarize, the SA-DCT in [2] thus efficiently fuses a DCT-based filtering and the result of a segmentation applied on the deblurred input image by a Wiener filtering. The segmentation used in this method (as in [3]) implicitly exploits an image prior model expressing that any real-world images can be approximated by an union of a number of nonoverlapping and distinct regions (of uniform grey level value). By comparison, our restoration algorithm aims at fusing a DCT-based sparsity and an edge preserving GGMRF constraints which favors edge sparsity in the recovered image in order to doubly regularize an iterative deconvolution procedure.

TABLE III

PERFORMANCE COMPARISON BETWEEN OUR ALGORITHM AND OTHER RESTORATION METHODS FOR EXPERIMENTS EXP5-6

	ISNR (dB)	
Methods	Exp5	Exp6
GGMRF-DCT-gradient	**3.99**	**2.96**
DCT-gradient	3.93	2.75
GGMRF-gradient	3.35	2.47
(2008) Mignotte [4]	**4.24**	2.99
(2006) Mignotte [3]	3.50	1.90
(2000) Molina *et al.* [32]	-	2.22 (PSNR=21.1)
(1998) May *et al.* [33]	3.43	-
(1997) Charbonnier *et al.* [34] (in [32])	-	1.86 (PSNR=20.8)

The performance of the SA-DCT regularized deconvolution algorithm depends on two regularization parameters (ϵ_1 and ϵ_2) which are manually tuned and are different for each experiment. Respectively $(0.013, 0.040)$, $(0.038, 0.045)$, $(0.062, 0.030)$ and finally $(0.10, 0.12)$ are chosen in [2] by the authors for Exp1, Exp2, Exp3 and Exp4 and are optimal for these experiments (see the Matlab procedure demo_SADCT_deblurring_copy.m available on-line at http address given in [2]). By comparison, our restoration method relies on one regularization function (see Eq. (6)) which is the same for all images and degradation models.

D. Discussion

Table IV shows the time in seconds and the number of iterations that each restoration took for each one of the considered degradation models according Eq. (10) (cf. Table I) and for our algorithm (cf. Algorithm II) (system used: AMD Athlon 64 Processor 3500+, 2.2 GHz, 4435.67 bogomips and non-optimized code running on Linux). Source code (in C++ language) of our algorithm (with the set of initial, degraded and restored images) are publicly available at the following http address www.iro.umontreal.ca/∼mignotte/ ResearchMaterial/sfrbr.html in order to make possible eventual comparisons with future restoration methods. Let us notice that our restoration procedure could be computationally optimized since numerous fast Very Large Scale Integration (VLSI) chips exist for computing more quickly the DCT transform.

Fig. 3 shows the evolution of the ISNR and its convergence as a function of the number of iterations for respectively the degradation models Exp3 and Exp4.

We can notice that the proposed method leads to competitive restoration results for various level of blur and noise degradations in benchmark tests and gives a good compromise between restoration results for the high and low BSNR case. Besides, the proposed restoration method, combining the GGMRF and DCT constraints always significantly improves the ISNR result comparatively to a single GGMRF or DCT prior model in all the considered degradation models. This tends to demonstrate the ability of our strategy to efficiently fuse these two different constraints on the restoration result.

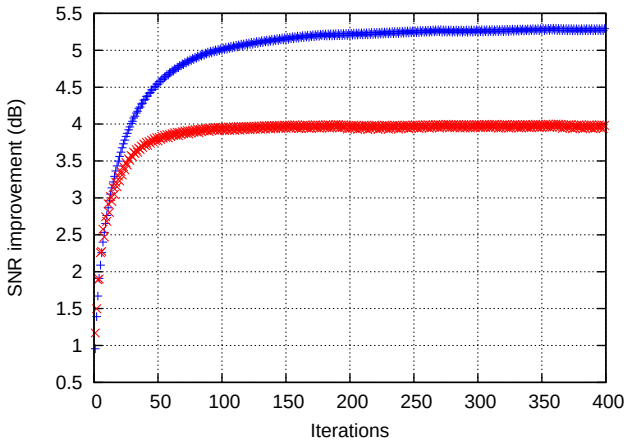

Fig. 3. Evolution of the SNR improvement for the CAMERAMAN image with the Exp3 and Exp5 degradation models.

Figures 1 and 2 show visually some restorations results for Exp1 and Exp3[2]. Let us also add that the estimation of T (which then ensures the estimation of γ) and the number of iterations could be improved since better ISNR results can be found if we supervised (by manually tuning) these two values for each tested experimental result presented in this paper.

The soft thresholding rule (Step 2. Algorithm 1) does not allow to improve the ISNR results compared to the hard thresholding rule used in our GGMRF-DCT-based restoration procedure. The ISNR results for the different experiments are equivalent or less good. More precisely, we respectively obtain for the different experiments; Exp1 : 7.35 dB Exp2 : 7.25 dB Exp3 : 5.08 dB Exp4 : 3.88 dB Exp5 : 3.51 dB Exp6 : 2.91 dB.

IV. Conclusion

In this paper, we have presented an efficient and simple doubly regularized restoration procedure combining efficiently two different edge-preserving regularization strategies respectively expressed in the spatial and frequential domains. Thanks to an adaptive and rescaling scheme, used to balance the influence of these two different regularizers, the resulting restoration strategy performs competitively among the recently reported state-of-the-art restoration schemes for different BSNR, blur and noise levels, while being simple to implement. This fusion of regularization terms can be a simple way to better model the intrinsic and complex properties of the original undegraded image to be recovered by simultaneously incorporating different types of knowledge concerning the types of restorations *a priori* defined as acceptable solutions.

References

[1] G. Chantas, N. Galatsanos, and A. Likas, "Bayesian restoration using a new nonstationary edge-preserving image prior," *IEEE Trans. Image Processing*, vol. 15, no. 10, pp. 2987–2997, 2006.

[2]Additional examples (i.e., degraded and restored image results) are also given in http: www.iro.umontreal.ca/∼mignotte/ ResearchMaterial/sfrbr.html

TABLE IV
TIME IN SECONDS AND ITERATION NUMBER FOR EXP1-6

	Time (sec)	Iterations
Exp1	525	4869
Exp2	117	750
Exp3	62	400
Exp4	78	400
Exp5	74	400
Exp6	1068	400

[2] A. Foi, K. Dabov, V. Katkovnik, and K. Egiazarian, "Shape-adaptive DCT for denoising and image reconstruction," in *Proceeding of SPIE Electronic Imaging 2006, Image Processing: Algorithms and Systems V*, vol. 6064A-18, http://www.cs.tut.fi/∼foi/SA-DCT/, January 2006.

[3] M. Mignotte, "A segmentation-based regularization term for image deconvolution," *IEEE Trans. Image Processing*, vol. 15, no. 7, pp. 1973–1984, 2006.

[4] ——, "A non-local regularization strategy for image deconvolution," *Pattern Recognition Letters*, vol. 29, no. 16, pp. 2206–221, December 2008.

[5] R. Neelamani, H. Choi, and R. Baraniuk, "ForWaRD: Fourier-wavelet regularized deconvolution for ill-conditioned systems," *IEEE Trans. Signal Processing*, vol. 52, no. 2, pp. 418–433, 2004.

[6] M. R. Banham and A. K. Katsaggelos, "Spatially adaptive wavelet-based multiscale image restoration," *IEEE Trans. Image Processing*, vol. 5, no. 4, pp. 619–634, 1996.

[7] J. Oliveira, J. Bioucas-Dias, and M. Figueiredo, "Adaptive total variation image deblurring: A majorization-minimization approach," *Signal Processing*, vol. 89, no. 9, pp. 1683–1693, September 2009.

[8] J. A. Guerrero-Colon and J. Portilla, "Deblurring-by-denoising using spatially adaptive gaussian scale mixtures in overcomplete pyramids," in *IEEE International Conference on Image Processing (ICIP'06)*, vol. I, Atlanta, GA, USA, October 2006, pp. 625–628.

[9] J. Bioucas-Dias, M. Figueiredo, and J. Oliveira, "Adaptive total-variation image deconvolution: A majorization-minimization approach," in *Proceeding of EUSIPCO'2006*, Florence, Italy, September 2006.

[10] ——, "Total variation image deconvolution: A majorization-minimization approach," in *IEEE International Conference on Acoustics, Speech, and Signal Processing (ICASSP'2006)*, vol. II, Toulouse, French, May 2006.

[11] M. Figueiredo and R. Nowak, "A bound optimization approach to wavelet-based image deconvolution," in *IEEE International Conference on Image Processing (ICIP'05)*, vol. II, Genova, Italy, September 2005, pp. 782–785.

[12] J. Bioucas-Dias, "Bayesian wavelet-based image deconvolution: a GEM algorithm exploiting a class of heavy-tailed priors," *IEEE Trans. Image Processing*, vol. 15, no. 4, pp. 937–951, 2006.

[13] M. A. T. Figueiredo and R. D. Nowak, "An EM algorithm for wavelet-based image restoration," *IEEE Trans. Image Processing*, vol. 12, no. 8, pp. 906–916, 2003.

[14] G. Chantas, N. P. Galatsanos, and A. Likas, "Bayesian image restoration based on variational inference and a product of student-t priors," in *Proceedings of the IEEE International MLSP Workshop*, Thessaloniki, Greece, August 2007.

[15] G. Chantas, N. Galatsanos, A. Likas, and M. Saunders, "Variational bayesian image restoration based on a product of t-distributions image prior," *IEEE Trans. Image Processing*, vol. 17, no. 10, pp. 1795–1805, 2008.

[16] S. Haykin, *Neural Networks: A comprehensive Foundation*. Prenctice Hall, Inc., 1999.

[17] T. Dietterich, "Ensemble methods in machine learning," in *Proceedings of the First International Workshop on Multiple Classifier Systems, LNCS, Multiple Classifier Systems*, L. N. I. C. Science, Ed., vol. 1857. Springer, 2000, pp. 1–15.

[18] C. A. Bouman and K. Sauer, "A unified approach to statistical tomography using coordinate descent optimization," *IEEE Trans. Image Processing*, vol. 5, no. 3, pp. 480–492, 1996.

[19] ——, "A generalized Gaussian image model for edge-preserving MAP estimation," *IEEE Trans. Image Processing*, vol. 2, no. 3, pp. 296–310, 1993.

[20] B. J. Sullivan and H.-C. Chang, "A generalized landweber iteration for ill-conditioned signal restoration," in *IEEE International Conference on Acoustics, Speech, and Signal Processing (ICASSP'91)*, Toronto, Ontario, Canada, April 1991, pp. 1729–1732.
[21] L. Landweber, "An iterative formula for fredholm integral equations of the first kind," *American Journal of Mathematics*, vol. 73, pp. 615–624, 1951.
[22] E. Simoncelli, "Bayesian denoising of visual image in the wavelet domain," *Bayesian Inference in Wavelet Based Models. eds. P. Mller and B. Vidakovic. Springer-Verlag, Lecture Notes in Statistics 141*, March 1999.
[23] D. L. Donoho and I. M. Johnstone, "Ideal spatial adaptation by wavelet shrinkage," *Biometrika*, vol. 81, pp. 425–455, December 1994.
[24] H. S. Malavar, *Signal Processing with Lapped Transforms*. Norwood, MA, Artech House, 1992.
[25] R. Coifman and D. Donohu, "Translation invariant denoising," in *Wavelets and Statistics*, *Lecture Notes in Statistics*, vol. 103. A. Antoniadis and G. Oppenheim, Eds. New York:Springer-Verlag, 1995, pp. 125–150.
[26] T. Ooura, "General purpose FFT (fast fourier/cosine/sine transform) package," http://momonga.t.u-tokyo.ac.jp/∼ooura/fft.html.
[27] K. Dabov, A. Foi, V. Katkovnik, and K. Egiazarian, "Image restoration by sparse 3d transform-domain collaborative filtering," in *Proceedings of SPIE, the International Society for Optical Engineering Image Processing: Algorithms and Systems VI*, vol. 6812-07, San Jose, CA, USA, January 2008.
[28] S. D. Babacan, R. Molina, and A. K. Katsaggelos, "Total variation image restoration and parameter estimation using variational distribution approximation," in *International Conference on Image Processing (ICIP'07)*, vol. I, San Antonio, Texas, USA, September 2007, pp. 97–100.
[29] V. Katkovnik, A. Foi, K. Egiazarian, and J. Astola, "Directional varying scale approximations for anisotropic signal processing," in *Proceedings of XII European Signal Processing Conference, EUSIPCO 2004,*, Vienna, Austria, 2004, pp. 101–104.
[30] A. Jalobeaunu, N. Kingsbury, and J. Zerubia, "Image deconvolution using hidden Markov tree modeling of complex wavelet packets," in *IEEE International Conference on Image Processing (ICIP'01)*, vol. I, Thessaloniki, Greece, October 2001, pp. 201–204.
[31] J. Liu and P. Moulin, "Complexity-regularized image restoration," in *IEEE International Conference on Image Processing (ICIP'98)*, vol. I, Chicago, Illinois, USA, October 1998, pp. 555–559.
[32] R. Molina, A. K. Katsaggelos, J. Mateos, A. Hermoso, and C. A. Segall, "Restoration of severely blurred high range images using stochastic and deterministic relaxation algorithms in compound Gauss-Markov random fields," *Pattern Recognition*, vol. 33, no. 4, pp. 555–571, 2000.
[33] K. May, T. Stathaki, A. G. Constantinides, and A. K. Katsaggelos, "Iterative determination of local bound constraints in iterative image restoration," in *IEEE International Conference on Image Processing (ICIP'98)*, vol. II, Chicago, Illinois, USA, October 1998, pp. 833–836.
[34] P. Charbonnier, L. Blanc-Feraud, G. Aubert, and M. Barlaud, "Deterministic edge-preserving regularization in computed imaging," *IEEE Trans. Image Processing*, vol. 5, no. 12, pp. 298–311, 1997.